MOLECULAR AND CELLULAR BIOLOGY, Feb. 1999, p. 1369–1380 Vol. 19, No. 2
0270-7306/99/$04.00+0

Control of *Saccharomyces cerevisiae* Filamentous Growth by Cyclin-Dependent Kinase Cdc28†

NICHOLAS P. EDGINGTON,‡ MELISSA J. BLACKETER, TRACIE A. BIERWAGEN, AND ALAN M. MYERS*

Department of Biochemistry and Biophysics, Iowa State University, Ames, Iowa 50011

Received 16 July 1998/Returned for modification 6 October 1998/Accepted 26 October 1998

The ascomycete *Saccharomyces cerevisiae* exhibits alternative vegetative growth states referred to as the yeast form and the filamentous form, and it switches between the two morphologies depending on specific environmental signals. To identify molecules involved in control of morphologic differentiation, this study characterized mutant *S. cerevisiae* strains that exhibit filamentous growth in the absence of the normal external signals. A specific amino acid substitution in the cyclin-dependent protein kinase Cdc28 was found to cause constitutive expression of most filamentous growth characteristics. These effects include specifically modified cell polarity characteristics in addition to the defined shape and division cycle alterations typical of the filamentous form. Several other mutations affecting Cdc28 function also had specific effects on filamentous growth. Constitutive filamentous growth resulting from deletion of the protein kinase Elm1 was prevented by modification of Cdc28 such that it could not be phosphorylated on tyrosine residue 19. In addition, various mutations affecting Hsl1 or Swe1, known or presumed components of a protein kinase cascade that mediates Cdc28 phosphorylation on Y19, either prevented or enhanced filamentous growth. The data suggest that a protein kinase cascade involving Elm1, Hsl1, and Swe1 can modulate Cdc28 activity and that Cdc28 in turn exerts global effects that cause filamentous growth.

During vegetative growth, the ascomycete *Saccharomyces cerevisiae* is able to adopt one of two distinct morphologic forms (for a review, see reference 31), designated the yeast form and the filamentous form. Two distinct signaling regimes induce the filamentous form in wild-type cells. In the phenomenon known as pseudohyphal growth, diploid cells become filamentous when grown on solid agar medium containing a rich carbon source but limited for nitrogen (26). Haploid cells also become filamentous but in response to a different signal. This phenomenon, known as invasive growth, occurs under the surface of mature colonies on rich agar medium (55).

The filamentous form is similar in invasive and pseudohyphal growth (26, 32, 55). Filamentous-form cells are significantly elongated compared to the yeast form, and cell separation after cytokinesis is delayed. Cell polarity is altered in the filamentous form, such that a daughter cell's initial bud is located nearly exclusively at the pole opposite the previous cytokinesis site. In contrast, in the yeast form, bud growth usually occurs adjacent to the previous site of cell division (22). Filamentous-form cells can grow invasively beneath the surface of agar media, whereas yeast-form cells grow exclusively on the surface of agar plates.

Yeast- and filamentous-form cells also differ in cell cycle control (32). In the yeast form, new daughter cells (i.e., cells that have not budded previously) expand isotropically during G_1 before initiating the formation of a new bud; after reaching a critical size, the Start checkpoint is passed and bud emergence occurs (for reviews, see references 36 and 53). After passing Start, cells are able to enter mitosis and complete cell division independent of bud size. Thus, the major control of cell division cycle progression is in G_1. The filamentous form differs in that buds emerge on new daughter cells very soon after cytokinesis without an intervening G_1 phase (32). Thus, in filamentous-form cells, the G_1 size requirement either is no longer operative or is already satisfied in the incipient new cell at the time of cytokinesis. Despite the complexity of this process, there is a simple visual indication of the difference in cell cycle progression, which is that buds emerge simultaneously in mother-daughter pairs in the filamentous form. The yeast form differs in that the mother cell usually forms a bud before the daughter cell, indicative of faster passage of Start. The apparent differences in cell division control in the filamentous form suggest involvement of the cyclin-dependent protein kinase (CDK) Cdc28, which is a central regulatory factor in determining whether *S. cerevisiae* passes several different cell cycle control points (for reviews, see references 23, 50, and 73).

Many factors are known to be involved in filamentous-growth signaling. These include a potential nutrient-sensing ammonia transporter (41); a trimeric G protein (33, 40); upstream regulators of a mitogen-activated protein (MAP) kinase cascade including Ras2, Ste20, and 14-3-3 proteins (26, 46, 47, 56); the Ste MAP kinase cascade; its transcription factor target, Ste12, and regulators thereof (16, 37, 43, 44, 55, 66); and other putative transcription factors (13, 24, 25, 38, 70). Despite this body of knowledge, little is known about the targets of these pathways that mediate the changes in the filamentous form, although the flocculin protein Flo11 has recently been identified as a possible candidate (39). As a potential means of identifying downstream target molecules, mutant strains were analyzed that constitutively exhibit elongated cell morphology and other specific filamentous-form characteristics independent of the signal that normally is required for morphologic differentiation in wild-type cells (8–10). One of the genes identified in this screen, *ELM1*, codes for a serine/threonine protein kinase (30). Deletion of *ELM1*

* Corresponding author. Mailing address: Department of Biochemistry and Biophysics, 2110 Molecular Biology Building, Iowa State University, Ames, IA 50011. Phone: (515) 294-9548. Fax: (515) 294-0453. E-mail: ammyers@iastate.edu.

† Journal paper J-18199 of the Iowa Agriculture and Home Economics Experiment Station, Ames, from project 3197.

‡ Present address: Cold Spring Harbor Laboratory, Cold Spring Harbor, NY 11724.

causes constitutive filamentous growth independent of the growth medium, surface contact, or cell ploidy (8), suggesting that Elm1 functions as a downstream regulator of morphologic differentiation. The targets of Elm1 that may be responsible for changes in cellular growth are not known. Another gene identified in this way, *ELM7*, was suggested to play a central role because of its extensive genetic interactions with other mutations affecting cell morphology (10).

Through further characterization of *ELM7* and *ELM1*, this study describes two lines of evidence indicating that Cdc28 function is a controlling factor in the decision to grow in the filamentous or yeast form. First, a specific mutation altering Cdc28 function was identified that constitutively causes most of the filamentous-form characteristics, including cell shape and polarity in addition to cell cycle parameters. Second, several elements of the protein kinase cascade that phosphorylates Cdc28 on tyrosine 19 were found to regulate filamentous growth, both as potential downstream regulators of the effects of Elm1 and in otherwise wild-type cells exposed to the invasive growth regime. The data support the hypothesis that modulation of Cdc28 function in response to environmental signals is in large part responsible for the transition between the yeast form and the filamentous form.

MATERIALS AND METHODS

Media and strain construction. The *S. cerevisiae* strains used in this study are listed in Table 1. Standard genetic methods were used for mating of *S. cerevisiae* strains, selection of diploids, induction of meiosis, and tetrad dissection (57). *S. cerevisiae* transformation was carried out by the lithium acetate procedure (3). One-step gene replacement and targeted integration of prototrophic markers into the *S. cerevisiae* genome were performed as described previously (58). Gene replacement was confirmed by DNA gel blot analysis and/or by the obvious appearance of the specific phenotype known to result from deletion of the gene undergoing modification (data not shown). Standard rich (YPD) and synthetic (SD) agar (2%) media were used as described previously (57). Unless otherwise noted, media contained 2% glucose as the carbon source.

Isolation and genetic analysis of suppressor mutations. Derivatives of *elm1-1* strain 104D576b that exhibited yeast-form morphology were identified by visual screening following transformation with a plasmid library. Ten of these remained in the yeast form independent of any transforming plasmid. The elongated-morphology phenotype was readily recovered in progeny of crosses to a wild-type tester strain, indicating in each instance an extragenic suppressor mutation (generically termed *sel*). Dominance or recessiveness was determined by mating each original isolate to *elm1-1* strain 104D6. Tetrads from these diploids invariably produced two spore clones with typical yeast-form cell morphology and two with the filamentous-form characteristics typical of *elm1-1* strains, indicating that the suppression phenotype is a single-gene trait. Segregants from these crosses of the genotype *MAT*α *ura3 elm1-1 sel* were collected for each original isolate. These were used to determine allelism relationships of the 10 *sel* mutations by genetic linkage. Each segregant was mated to each original isolate (*MAT***a** *leu2 elm1-1 sel*). Allelism was assigned if yeast form colonies were observed exclusively in the progeny of such a cross, whereas nonallelic mutations were indicated by recovery of colonies with filamentous form characteristics typical of *elm1-1* strains; at least 30 complete tetrads were examined for each cross. An allelic group of five dominant mutations defined the locus originally designated *SEL2* and subsequently identified as *HSL1*.

Construction of plasmids containing *CDC28*, *cdc28-127*, or *cdc28-Y19F*. Standard molecular biology methods were used for PCR amplification and plasmid construction (3, 61, 63). *CDC28* was obtained from D. Lew (Duke University) as a 2.03-kb fragment extending from the *Xho*I site 342 bp upstream of the initiation codon to the *Pvu*II site 790 bp downstream of the termination codon. This fragment contains a 2-bp stretch inserted immediately upstream of the *CDC28* initiation codon that create an *Nde*I site not present in the native gene. This *CDC28* fragment was cloned in the *Xho*I and *Sma*I sites of pRS306, pRS316, or pRS305 to construct p28WT-URAi, p28WT-URAc, and p28WT-LEUi, respectively. Plasmid p28MUT-URAc, containing the allele *cdc28-127*, was constructed by replacing the region between the unique *Eco*NI and *Hin*dIII sites of p28WT-URAc with the equivalent region from a fragment amplified by PCR from genomic DNA of a *cdc28-127* haploid strain.

Plasmid p28Y19F-URAc, carrying *cdc28-Y19F*, was constructed as follows. Oligonucleotide primer 1022R from the noncoding strand of *CDC28* contains a missense mutation that changes tyrosine codon 19 (TAC) to a phenylalanine codon (TTC). This primer was used to amplify by PCR a 126-bp region extending from 60 bp upstream of the *CDC28* initiation codon to codon 22 of the open reading frame (ORF). The template for this reaction was p28WT-URAc. This small fragment was then extended by PCR to beyond the unique *Hin*dIII site within *CDC28*. The *Nde*I-*Hin*dIII fragment excised from the amplification product was used to replace the equivalent region of *CDC28* in p28WT-LEUi, forming plasmid p28Y19F-LEUi. The nucleotide sequence of the entire *CDC28* gene in p28Y19F-LEUi was determined, confirming the presence of the Y19F mutation. The only other changes from the wild-type sequence are a silent mutation changing codon 22 from GTA to GTT and also the mutation forming the *Nde*I site at the initiation codon. The *Xho*I-*Eco*NI fragment of p28Y19F-LEUi containing the Y19F mutation was used to replace the equivalent region of p28WT-URAc, forming plasmid p28Y19F-URAc.

***HSL1* plasmids.** *HSL1* was excised from phage clone ATCC71138 (American Type Culture Collection, Rockville, Md.) as a 7.26-kb *Bam*HI-*Sst*I fragment and cloned in pRS316 to form plasmid pNE30. The dominant *HSL1* allele designated *SEL2-1* was obtained by in vivo gap repair as follows. pNE30 was digested at the unique *Sun*I and *Nru*I sites within *HSL1*, which removes the entire ORF but leaves significant lengths of the 5′- and 3′-flanking sequences. The resulting linear fragment was used to transform the *SEL2-1* strain NEY2065 to uracil prototrophy. The autonomously replicating plasmid pNE30GR was recovered from one transformant after amplification in *Escherichia coli*. This plasmid was shown to have been repaired from the dominant allele *SEL2-1* by its ability to suppress the filamentous-growth characteristics of an *elm1-1* strain. Plasmid pNE33d is a *LEU2*-marked integrative plasmid that was constructed by excising the *Bam*HI-*Sst*I fragment bearing *SEL2-1* from pNE30GR and cloning it in pRS305.

Gene disruptions and tagging by integrative transformation. Recombinant DNA fragments used to replace wild-type alleles with deletion mutations were described previously for *elm1::HIS3* (8), *bud2*Δ*::LEU2* (52), *clb2::LEU2* (54), and *put3::URA3* (45). The fragment used to introduce *swe1::URA3* was constructed by digesting pSWE1-10g (11) with *Xba*I to remove the *LEU2* insert from *swe1::LEU2* and replacing that region with a 1.2-kb *Nhe*I fragment containing *URA3* (20). The resultant plasmid is p*swe1::URA3*, from which a 2.5-kb disruption fragment can be excised by digestion with *Hin*dIII and *Bam*HI. The *GFA1* locus was tagged with *URA3* as a selective marker by first cloning a genomic *Eco*RI fragment containing *GFA1* (71) in pRS306, linearizing the resultant plasmid at the unique *Sph*I site within *GFA1*, and then transforming strain NEY1489 to uracil prototrophy.

The deletion allele *hsl1::LEU2* was constructed as follows. A 5.34-kb *Pvu*II-*Sst*I fragment of the *HSL1* locus was excised from pNE30 and cloned in pUC118 digested with *Sma*I and *Sst*I. The entire *HSL1* ORF between the unique *Nru*I and *Sun*I sites was removed; after digestion with these two enzymes, the remaining plasmid was made blunt ended by treatment with DNA polymerase I Klenow fragment (polIK) and ligated to an *Nhe*I linker to form plasmid pNE37. The 2.2-kb *Xba*I fragment containing *LEU2* was excised from pSWE1-10g (11) and inserted into this unique *Nhe*I site to form plasmid pNE38. Digestion of this plasmid with *Sst*I and *Hin*dIII releases a 2.59-kb disruption fragment containing *hsl1::LEU2*.

The deletion allele *cdc28::LEU2a* was constructed as follows. The 2.03-kb *Xho*I-*Pvu*II genomic DNA fragment containing *CDC28* was cloned in the *Xho*I and *Sma*I sites of pBluescript SK(+). The region of *CDC28* between the unique *Nde*I and *Hin*dIII sites (codons 1 to 247) was replaced with the *LEU2* gene obtained as a 2.8-kb *Bgl*II fragment from plasmid YEp13 (12). To facilitate this cloning step, the *Nde*I-*Hin*dIII-cleaved *CDC28* plasmid was made blunt ended by treatment with polIK and ligated to a *Bgl*II linker. The resultant plasmid, pCdc28::LEU2, provides *cdc28::LEU2a* as a 4.1-kb fragment excised by digestion with *Apa*I and *Bam*HI.

Size measurements and estimation of cell volume. Random fields of 30 to 50 cells were captured for analysis as digital files by using the program NIH Image; all unbudded and singly budded mother cells were measured. Cell volumes were estimated by assuming that the cell shape approximated a prolate spheroid and applying the formula $V = (4/3)\pi(a/2)(b/2)^2$, where a is the length of the cell and b is the maximum width. At least 200 cells were analyzed for each genotype characterized.

Determination of bud site selection. A segregating population was generated by crossing strain 127D6 (*cdc28-127*) to strain **a**DL (*CDC28*) and collecting progeny clones from complete tetrads. Wild-type and mutant siblings, along with the parental strains, were analyzed by time-lapse photography to determine directly the location of bud emergence sites and the relative timing of bud emergence on mother-daughter cell pairs. For this analysis, cells were first grown overnight on rich agar medium. Small-budded cells then were dragged to a new location on the plate by using a micromanipulator. The position of mother cells and their buds was noted. Images of the cells were captured immediately after micromanipulation and at approximately 1-h intervals thereafter. For the parental strains, at least 100 cell divisions were examined for bud site selection. For progeny clones, 32 divisions or more were characterized. A minimum of 10 independent progeny clones of each type were analyzed.

The effect of *clb2::LEU2* on bud site selection was determined similarly with strain AY2249 (*clb2::LEU2*) and progeny of this strain crossed to strain 127D5 (*cdc28-127*); only progeny strains bearing the wild-type *CDC28* allele were analyzed. The effect of *bud2*Δ*::LEU2* on bud site selection in *cdc28-127* strains was analyzed in progeny of a cross between strain AY102X (*bud2*Δ*::LEU2*) and strain 127D5 (*cdc28-127*). Seven *cdc28-127 bud2*Δ*::LEU2* progeny and five

TABLE 1. *S. cerevisiae* strains used in this study

Strain[a]	Genotype	Reference, source, or derivation
W303	*MAT***a**/*MAT*α *ura3/ura3 leu2/leu2 his3/his3 ade2/ade2 trp1/trp1*	69
W303-1A	*MAT***a** *ura3 leu2 his3 ade2 trp1*	69
ΣΣ	*MAT***a**/*MAT*α *ura3/ura3 leu2/leu2*	L5487 × L5684[b]
DDUL	*MAT***a**/*MAT*α *ura3/ura3 leu2/leu2 his3/+*	This study
αDUL	*MAT*α *ura3 leu2*	This study
αDU	*MAT*α *ura3*	This study
aDUL	*MAT***a** *ura3 leu2*	This study
aDL	*MAT***a** *leu2*	This study
NEY2158	*MAT***a** *ura3 leu2 his3*	This study
NEY2159	*MAT*α *ura3 leu2 his3*	This study
104D6	*MAT*α *ura3 elm1-1*	10
104D576b	*MAT***a** *leu2 met6 elm1-1*	10
104DP10c	*MAT***a** *ura3 his3 elm1-1*	This study
NEDN6d	*MAT*α *ura3 leu2 met6 elm1-1*	10
NEY1489	*MAT***a** *ura3 leu2 met6 elm1-1*	10
127D6	*MAT*α *ura3 cdc28-127*	10
127D5	*MAT***a** *leu2 cdc28-127*	10
AY2287	*MAT***a** *ura3 leu2 cdc28-127*	127D6 × **a**DL
AY2285	*MAT***a** *ura3 leu2*	127D6 × **a**DL
AY100X	*MAT***a** *ura3 leu2 CDC28-URA3*	Transformation of **a**DUL with p28WT-URAi
AY101X	*MAT***a** *leu2 cdc28-127*	127D6 × **a**DL
AY102X	*MAT*α *ura3 leu2 bud2*Δ*::LEU2*	Transformation of αDUL
AY2241	*MAT*α *cdc28-127 bud2*Δ*::LEU2 leu2*	Segregant of AY102X × AY2287
AY2242	*MAT*α *cdc28-127 BUD2 leu2*	Segregant of AY102X × AY2287
AY2249	*MAT*α *ura3 leu2 clb2::LEU2*	Transformation of αDUL
AY2252	*MAT***a** *ura3 cdc28-127 leu2-GAL::CLB2-LEU2*	Transformation of AY2287 with YIpG2::CLB2[c]
AY2305	*MAT***a**/*MAT*α *CDC28/cdc28::LEU2a ura3/ura3 leu2/leu2 his3/+*	Transformation of DDUL
AY2153	*MAT*α *cdc28::LEU2a ura3 leu2* (p28MUT-URAc)	Segregant of AY2305 transformant
AY2399	*MAT*α *ura3 leu2 his3 cdc28::LEU2a* (p28Y19F-URAc)	Segregant of AY2305 transformant
WW28Δ/+	*MAT***a**/*MAT*α *CDC28/cdc28::LEU2a ura3/ura3 leu2/leu2 his3/his3 trp1/trp1 ade2/ade2*	Transformation of W303
Y2195	*MAT*α *cdc28::LEU2a ura3 leu2 his3 trp1 ade2* (p28MUT-URAc)	Segregant of WW28Δ/+ transformant
Y2194	*MAT*α *cdc28::LEU2a ura3 leu2 his3 trp1 ade2* (p28WT-URAc)	Segregant of WW28Δ/+ transformant
ΣΣ28Δ/+	*MAT***a**/*MAT*α *CDC28/cdc28::LEU2a ura3/ura3 leu2/leu2*	Transformation of ΣΣ
AY2204	*MAT*α *cdc28::LEU2a ura3 leu2 his3 trp1 ade2* (p28MUT-URAc)	Segregant of ΣΣ28Δ/+ transformant
NEY2170	*MAT***a** *leu2 ura3 his3 elm1::HIS3*	Transformation of NEY2158
AY2451	*MAT***a** *leu2 ura3 his3 elm1::HIS3 cdc28::LEU2a* (p28Y19F-URAc)	Segregant of AY2399 × NEY2170
AY2452	*MAT***a** *leu2 ura3 his3 elm1::HIS3 CDC28* (p28Y19F-URAc)	Segregant of AY2399 × NEY2170
NEY1494	*MAT***a** *leu2 met6 elm1-1 SEL2-1*	Mutation of 104D576b
NEY2018	*MAT***a** *ura3 his3 elm1-1 put3::URA3*	Transformation of 104DP10c
NEY2019	*MAT*α *ura3 leu2 met6 elm1-1 bud2*Δ*::LEU2*	Transformation of NEDN6d
NEY2020	*MAT***a** *ura3 leu2 met6 elm1-1 GFA1:URA3*	Transformation of NEY1489
NEY2065	*MAT*α *ura3 elm1-1 SEL2-1*	Segregant from NEDN6d × NEY1494
NEY2170	*MAT***a** *ura3 leu2 his3 elm1::HIS3*	Transformation of NEY2158
NEY100X	*MAT*α *ura3 leu2 his3 sel2::LEU2*	Transformation of NEY2159
NEY2299	*MAT***a** *ura3 leu2 his3 elm1::HIS3 swe1::URA3*	Transformation of NEY2170
NEY2317	*MAT***a**/*MAT*α *ura3/ura3 leu2/leu2 his3/his3 elm1::HIS3/+ sel2::LEU2/+ swe1::URA3/+*	NEY2299 × NEY100X
NEY2335	*MAT***a** *ura3 leu2 his3 sel2::LEU2*	Progeny of NEY2317
NEY2338	*MAT***a** *ura3 leu2 his3 elm1::HIS3*	Progeny of NEY2317
NEY2339	*MAT*α *ura3 leu2 his3 sel2::LEU2 swe1::URA3*	Progeny of NEY2317
NEY2340	*MAT***a** *ura3 leu2 his3*	Progeny of NEY2317
NEY2341	*MAT*α *ura3 leu2 his3 elm1::HIS3 swe1::URA3*	Progeny of NEY2317
NEY2344	*MAT*α *ura3 leu2 his3 swe1::URA3*	Progeny of NEY2317
NEY2353	*MAT***a** *ura3 leu2-SEL2-1-LEU2*	Integrative transformation of **a**DUL with pNE33d

[a] All strains are related to the parental reference strain D273-10B/A1 (68) by at least five backcrosses, unless otherwise noted as being derived from W303 or Σ.
[b] These parental strains in the Σ background were provided by C. Styles, Whitehead Institute.
[c] Provided by D. Lew, Duke University.

cdc28-127 BUD2 siblings were analyzed for bud position and cell shape; distinctions in these phenotypic parameters corresponded precisely to the genotype.

RESULTS

Characterization of *cdc28-127*. The mutation *elm7-1*, which constitutively displays multiple characteristics of the filamentous form (10) (Fig. 1A and B), was found to be an allele of *CDC28*. The wild-type allele of *elm7-1* was cloned by complementation of the cold-sensitive growth defect also caused by the mutation. One derivative strain able to grow at 15°C after transformation of an *elm7-1* mutant with a wild-type genomic DNA library also displayed the ovoid cell shape typical of yeast form cells. This strain contained plasmid p127c, which was

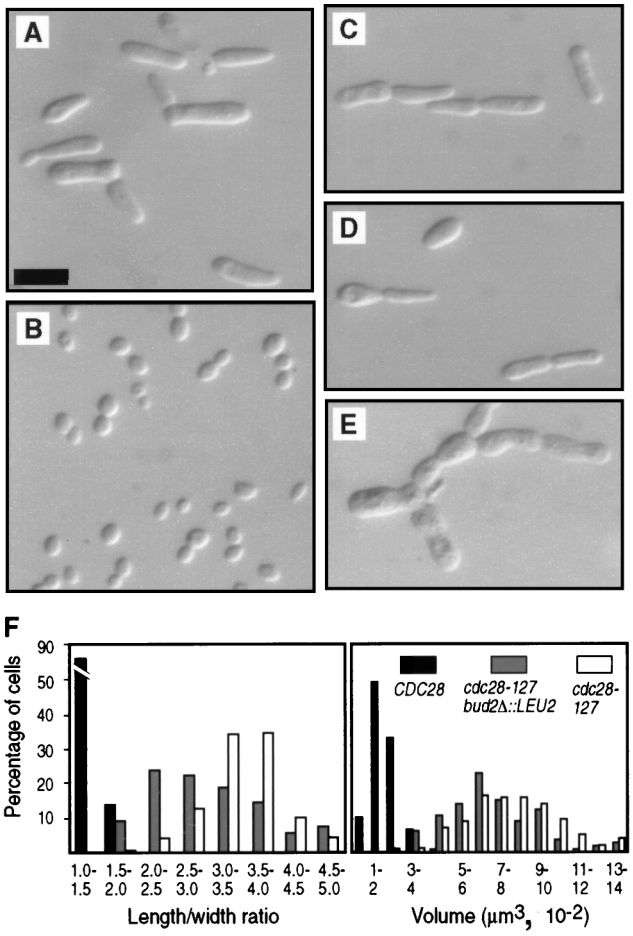

FIG. 1. Effects of *cdc28-127* on cell size and morphology. Haploid strains were grown overnight on YPD plates and photographed suspended in 1.2 M sorbitol. Bar, 10 μm. (A) Strain AY2287 (*cdc28-127*). (B) Strain AY2285 (*CDC28*). (C) Strain AY2153 (*cdc28-127* reconstructed in the D273-10B/A1 background). (D) Strain AY2204 (*cdc28-127* reconstructed in the Σ background). (E) Strain AY2195 (*cdc28-127* reconstructed in the W303 background). (F) Distribution of length/width ratios and approximate cell volumes. The *cdc28-127* and *CDC28* strains analyzed were AY2287 and AY2285 (A and B, respectively); the *cdc28-127 bud2Δ::LEU2* strain is AY2241 shown in Fig. 2C.

shown to be responsible for complementation of *elm7-1* by the fact that vegetative segregants lacking the plasmid regained both the abnormal cell shape and cold-sensitive growth phenotypes. Nucleotide sequence analysis revealed that the genomic insert in p127c contained *CDC28*. Plasmid p28WT-URAc, in which *CDC28* is the only intact genetic element in the insert DNA, was introduced into *elm7-1* strains and found to restore normal yeast form morphology, again in a plasmid-dependent manner (data not shown). Thus, *CDC28* complements *elm7-1* when present as part of a centromeric plasmid.

CDC28 was found to be genetically inseparable from the *elm7-1* mutation. The *URA3* gene was inserted as a marker into the genome adjacent to the wild-type *CDC28* locus in strain AY100X. This strain was crossed to the *elm7-1* mutant 127D6, and tetrads were analyzed. *CDC28* (indicated by uracil prototrophy) and *elm7-1* (indicated by elongated cell morphology) segregated in opposition in 30 complete tetrads, indicating tight linkage of the two genetic elements. The fact that *CDC28* both complements and is tightly linked to *elm7-1* indicates allelism. Accordingly, *elm7-1* here is renamed *cdc28-127*.

The specific mutation in *cdc28-127* that causes constitutive filamentous growth was found to be replacement of cysteine residue 127 by tyrosine (termed C127Y, and the mutant protein is designated $Cdc28^{C127Y}$). The *CDC28* locus was isolated from wild-type and *cdc28-127* strains by PCR amplification of genomic DNA. Nucleotide sequence analysis of several independent clones showed that *cdc28-127* differs from the wild-type allele *CDC28* only by the C127Y mutation. To prove that C127Y is the causative agent of the observed phenotypes, the mutant gene was used to replace *CDC28* in three different wild-type haploid genetic backgrounds, namely, D273-10B/A1, W303, and Σ. In all instances, the resultant strains displayed the morphologic and growth defects observed for the original *cdc28-127* mutant strain (Fig. 1C to E). The genetic background, however, had modifying effects on the particular cell morphology and also affected the growth rate. In the D273-10B/A1 background, *cdc28-127* strains grew on rich agar plates at a slightly reduced rate compared to congenic *CDC28* strains; in the W303 background, the mutant strains grew significantly slower than did the wild-type control strains; and in the Σ background, the mutant strains grew extremely slowly compared to the wild type, requiring 4 to 5 days at room temperature to form a colony that could be transferred to a fresh plate (data not shown).

Filamentous growth characteristics caused by *cdc28-127*. The mutation *cdc28-127* causes most of the known characteristics of filamentous form cells. The following observations were made on haploid strains grown to early exponential phase in liquid cultures of rich medium (YPD), implying that filamentous growth characteristics occur in the absence of the normal requirements for diploidy, nitrogen limitation, and contact with agar medium. Cells bearing *cdc28-127* were significantly elongated compared to congenic *CDC28* cells (Fig. 1F). Enhanced ability to grow invasively in rich agar medium was observed previously for a *cdc28-127* strain (10), and this was observed again in the *cdc28-127* mutants constructed by gene replacement (data not shown). Strains containing *cdc28-127* did not form large cell clumps during growth in liquid medium. Thus, the delayed cell separation phenotype characteristic of filamentous-form growth is not caused by *cdc28-127*.

The cell division cycle characteristics of filamentous-form growth also are caused by *cdc28-127*. In contrast to wild-type cells, mother-daughter pairs of *cdc28-127* mutants frequently contain buds very similar in size (Fig. 2A and B). Time-lapse photography commonly showed simultaneous bud emergence on mother-daughter pairs in *cdc28-127* strains (10) (Fig. 3A), whereas in congenic *CDC28* strains a bud almost always was visible on the mother cell prior to the daughter cell. In accordance with simultaneous bud emergence, measurement of DNA content per cell in asynchronous populations revealed that the frequency of cells in G_2 was significantly increased in a *cdc28-127* mutant compared to a congenic wild-type strain (Fig. 2D).

A possible explanation for this phenotype is that control of G_1 phase is modified in *cdc28-127* mutants so that cells pass Start and progress into S phase more rapidly than normal. An accelerated G_1 phase, however, normally causes reduced cell size. In contrast, *cdc28-127* mutant cells are significantly larger than congenic *CDC28* cells (Fig. 1F). Thus, some aspects of Cdc28 activity other than activation during G_1 are likely to be altered in the mutant.

The mutation *cdc28-127* also affects the mechanism of bud site selection, causing haploid cells to adopt the budding pattern typically observed in diploid cells of the pseudohyphal form. Bud site selection was determined by isolating cells with small buds on solid rich medium and observing in time-lapse photography the subsequent sites of bud emergence on moth-

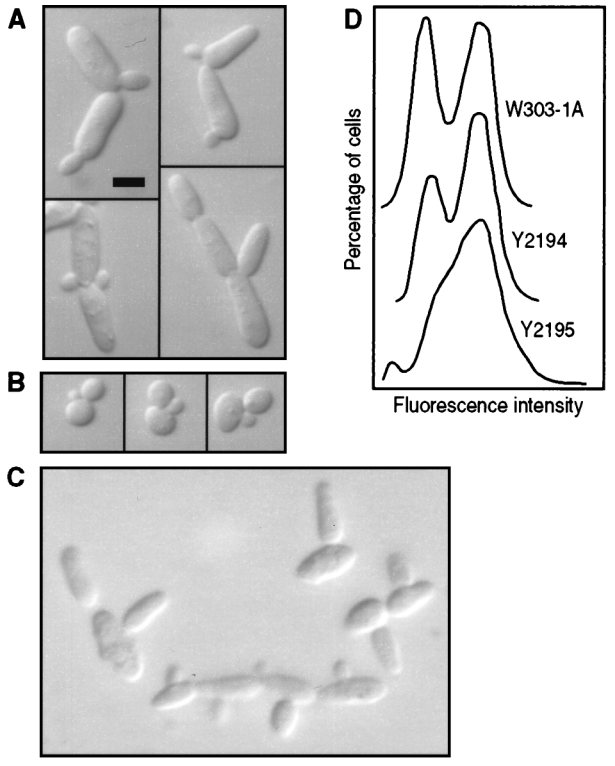

FIG. 2. Cell cycle parameters. Bar, 5 μm. (A) Strain AY2287 (*cdc28-127*). (B) Strain AY2285 (*CDC28*). (C) Strain AY2241 (*cdc28-127 bud2Δ::LEU2*). Cells were grown overnight in liquid YPD medium. (D) DNA content determined by fluorescence-activated cell sorter analysis (34). The indicated strains were converted to ρ^0 derivatives lacking mitochondrial DNA prior to analysis. Relevant genotypes are as follows: W303-1A, nonmutant; Y2194, *cdc28::LEU2a* (p28WT-URAc) (bearing *CDC28*); Y2195, *cdc28::LEU2a* (p28MUT-URAc) (bearing *cdc28-127*).

er-daughter cell pairs (Fig. 3). All strains analyzed were haploids; thus, the normal budding pattern is axial (i.e., both mother and daughter cells form buds adjacent to the previous cytokinesis site). As expected, axial budding was typical of wild-type control strains. Mutant cells always formed buds at one of the two poles of the elongated cells. Axial budding was comparatively rare in the mutants, however, which instead budded with high frequency in the bipolar budding pattern (i.e., both mother and daughter cells bud at the pole opposite the cytokinesis site) or in the unipolar budding pattern (i.e., daughter's first bud at the pole opposite the previous cytokinesis site, mother's next bud adjacent to that site). The unipolar budding pattern predominated over the bipolar pattern in the mutant cells (Fig. 3D). This distribution of bud site selection patterns cosegregated with the cell elongation phenotype in progeny of *cdc28-127*/*CDC28* diploid strains, indicating the alteration resulted specifically from *cdc28-127* and not from an unidentified mutation present in this genetic background.

***CDC28* affects bud site selection through known polarity establishment functions.** *CDC28* may affect bud site selection as an upstream regulator of the "polarity establishment functions" coded for by a large group of loci including the *BUD* genes (for reviews, see references 14 and 18). As an initial test of this hypothesis, *BUD2* was deleted in a haploid strain containing *cdc28-127*. Double-mutant progeny as well as *cdc28-127* and *bud2Δ::LEU2* single-mutant siblings were analyzed for bud site selection. As expected, bud site selection was primarily random in *bud2Δ::LEU2* strains (reference 15 and data not shown). In *cdc28-127 bud2Δ::LEU2* double-mutant strains, buds usually emerged from the longitudinal center of the elongated cells as opposed to the poles (Fig. 2C), a condition that was never observed in *BUD2 cdc28-127* siblings. Thus, the null mutation *bud2Δ::LEU2* is epistatic to *cdc28-127* regarding the bud site selection phenotype, consistent with the hypothesis that filamentous-form differentiation involves a specific Cdc28-mediated modification of the site selection functions.

The *BUD2* deletion mutation also affected the cell shape. The *cdc28-127 bud2Δ::LEU2* double mutants were significantly less elongated than the congenic *cdc28-127 BUD2* cells (Fig. 1F); this phenotype cosegregated with the *bud2* mutation in the progeny of a *bud2Δ::LEU2*/*BUD2 CDC28*/*cdc28-127* diploid (data not shown). The *bud2Δ::LEU2* mutation did not significantly affect the enlarged volume of *cdc28-127* cells (Fig. 1F). Thus, the general bud site selection functions may play an additional role in determination of cell shape in the growing bud.

Clb2 affects filamentous growth. The G_2-expressed cyclin Clb2 regulates cell shape (35), which suggests the hypothesis that $Cdc28^{C127Y}$ causes filamentous growth characteristics because of abnormal interaction with Clb proteins. To test this hypothesis *CLB2* first was deleted in a D273-10B/A1 haploid strain. A slight degree of cell elongation resulted, although the phenotype is much less severe than that caused by *cdc28-127* (Fig. 4A and B). A similar effect was observed in the haploid BF264-15DUa genetic background (54); however, a *clb2*/*clb2* diploid in this background displayed uniformly elongated cells similar to *cdc28-127* strains (35). Deletion of *CLB2* in haploid cells caused another phenotype that also results from *cdc28-127*, specifically, alteration of the budding pattern (Fig. 3B).

Cells bearing *cdc28-127* were shown to require Clb2 for viability, consistent with the hypothesis that $Cdc28^{C127Y}$ interacts abnormally with the G_2-expressed cyclins. *CLB2* requirement was indicated by analysis of tetrads from a *cdc28-127*/*CDC28 CLB2*/*clb2::LEU2* diploid (Fig. 4A to D). From this diploid, 11 of 14 tetrads were identified as tetratypes by the presence of one *cdc28-127 CLB2* progeny clone (elongated morphology, leucine auxotroph), one *CDC28 CLB2* progeny clone (wild-type morphology, leucine auxotroph), and one *CDC28 clb2::LEU2* progeny clone (slight cell elongation phenotype, leucine prototroph). In each instance, the fourth spore of the tetrad, predicted to carry both *cdc28-127* and *clb2::LEU2*, germinated but failed to develop a viable clone. Two of the tetrads contained two *CDC28 CLB2* progeny clones and two spores that did not form colonies; again the two inviable spores are predicted to be *cdc28-127 clb2::LEU2* double mutants. The terminal phenotype of germinating *clb2::LEU2 cdc28-127* spores suggests a lethal effect specifically in G_2, because large buds invariably were present (Fig. 4D).

Additional evidence suggesting that $Cdc28^{C127Y}$ is defective in its interaction with G_2 cyclins is that overexpression of *CLB2* suppressed the cell elongation phenotype caused by *cdc28-127*. The gene fusion *GAL::CLB2*, in which the *CLB2* coding sequence can be overexpressed from the *GAL* promoter, was integrated into the genome of a *cdc28-127* strain. Growth of this strain on galactose caused cells to revert to the normal ovoid shape typical of the yeast form (Fig. 4E and F). The carbon source had no effect on other *cdc28-127* strains in the absence of *GAL::CLB2* (data not shown).

Hsl1 affects filamentous-growth characteristics. An independent line of evidence implicating *CDC28* as a regulator of filamentous growth was provided by analysis of mutations that suppress the constitutive filamentous-growth phenotype induced by *elm1* mutations. Five allelic, dominant mutations were obtained in the locus designated *SEL2* (suppressor of

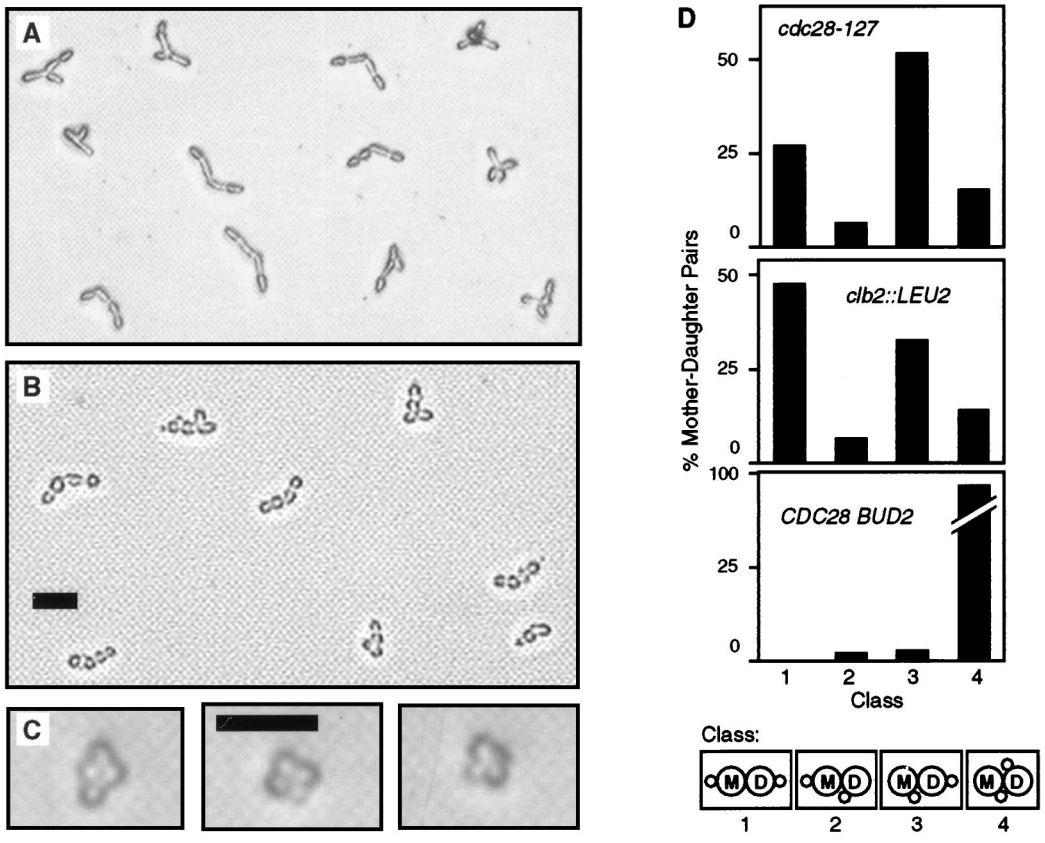

FIG. 3. Bud site selection. (A) Strain AY2287 (*cdc28-127*). (B) Strain AY2249 (*clb2::LEU2*). (C) Strain **a**DUL (*CDC28*). Cells are photographed on the surface of YPD agar medium. Bars, 25 μm. (D) Tabulation of data shown in panels A to C. Bud site selection classes are defined at the bottom of the panel.

elm1), each of which restores yeast-form morphology to *elm1-1* strains or those bearing *elm1* deletion mutations (data not shown; see Materials and Methods). *SEL2* was found to be linked to *ELM1* on chromosome XI, which enabled its cloning based on genetic map position. Genetic map distances from several cloned genes in the area were determined (Table 2), revealing that *SEL2* is located near ORF YKL101w. This ORF was subcloned in plasmid pNE30. The dominant mutant allele *SEL2-1* was rescued from the original suppressed strain for the purpose of testing whether YKL101w was in fact the locus responsible for suppression of *elm1-1*. The resultant gap-repaired plasmid, pNE30GR, was introduced into the parental *elm1-1* strain 104D576b. All transformants were completely restored to the yeast-form morphology (Fig. 5), indicating that YKL101w and *SEL2* are the same genetic element. YKL101w was previously designated *HSL1* or *NIK1* (42, 65), and thus *SEL2* will hereafter be referred to as *HSL1*.

Hsl1 is most similar to the protein kinase Nim1 from *Schizosaccharomyces pombe*; over a span of 304 aligned residues, 48% are identical in both proteins. The regions of high similarity are located within the protein kinase domains. *HSL1* comprises a reading frame of 1,519 codons, however; therefore, there are extensive regions outside of the protein kinase domain available to provide additional functions besides this catalytic activity. Nim1 is known to promote mitosis in *S. pombe* by inhibiting the activity of the tyrosine kinase Wee1, which in turn phosphorylates and inhibits the CDK Cdc2 (59, 60). In *S. cerevisiae*, the protein kinase Swe1 functions similarly to Wee1 downstream of Hsl1 (11, 42).

The fact that mutations of *HSL1* capable of suppressing *elm1-1* are dominant suggests that activation of Hsl1, predicted to result in inhibition of Swe1, is responsible for suppression of the constitutive filamentous-growth phenotype. From this hypothesis, it follows that inactivation of Hsl1, expected to result in hyperactivation of Swe1, would induce the filamentous form. Mutant strains bearing the deletion allele *hsl1::LEU2* were viable and did not show any obvious growth defects. The mutant cells were significantly elongated, however, and the budding pattern was switched in haploid cells from the normal axial pattern to the bipolar pattern (Fig. 6C). Both of these phenotypes were observed during growth in rich medium. Elongated cell morphology was found previously in *hsl1* mutants (42, 65), but in these strain backgrounds specific filamentous-growth characteristics were not evident.

The Swe1-Cdc28 pathway is required for induction of filamentous-growth characteristics by *elm1* or *hsl1* mutations. An *hsl1::LEU2 swe1::URA3* double mutant was constructed to test the hypothesis that the morphological effects of *HSL1* deletion are mediated by Swe1. The cell shape and budding-pattern phenotypes of this strain were typical of the yeast form (Fig. 6F), indicating that Swe1 is required for induction of filamentous-growth characteristics by the *hsl1* mutation. An *elm1::HIS3 swe1::URA3* double-mutant strain also was constructed, and again inactivation of *SWE1* suppressed the constitutive filamentous-growth phenotype (Fig. 6E).

The fact that elimination of Swe1 prevents filamentous-growth characteristics induced by *elm1* or *hsl1* mutations suggests that Y19 phosphorylation is necessary for the morphologic phenotype. This hypothesis was tested by replacing wild-type Cdc28 in an *elm1::HIS3* strain with a mutant form,

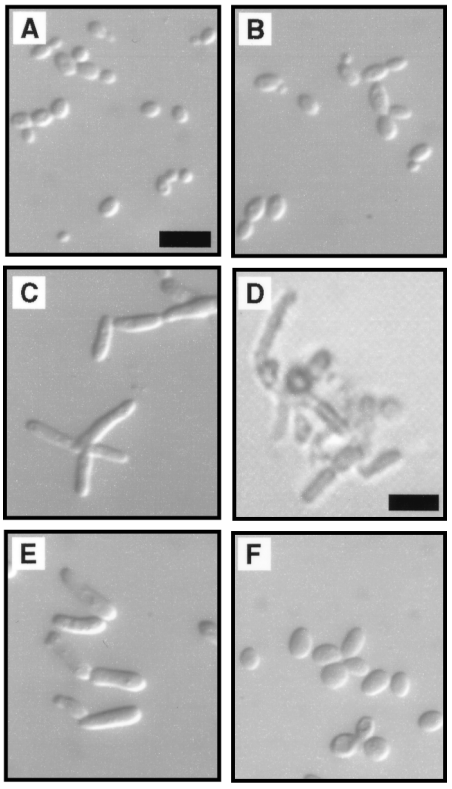

FIG. 4. Effects of altering *CLB2* expression in *cdc28-127* mutant strains. (A to D) Sibling progeny from the cross of strain AY2249 (*clb2::LEU2*) to strain AY101X (*cdc28-127*). Bars, 10 μm (A) and panel (D) 25 μm. Photomicrographs are of cells grown overnight on YPD plates and suspended on a slide in 1.2 M sorbitol, except for panel D, which shows a germinating spore clone after 2 days on YPD medium, observed under an inverted microscope. (A) *CDC28 CLB2*. (B) *CDC28 clb2::LEU2*. (C) *cdc28-127 CLB2*. (D) *cdc28-127 clb2::LEU2*. The clone shown in panel D did not develop further and is representative of 15 deduced *cdc28-127 clb2::LEU2* spores identified in tetratype and nonparental ditype tetrads from this cross. (E) Strain AY2252 (*cdc28-127 GAL:CLB2*) grown in YPD liquid medium to early log phase. (F) Strain AY2252 grown in YPGal liquid medium to early log phase.

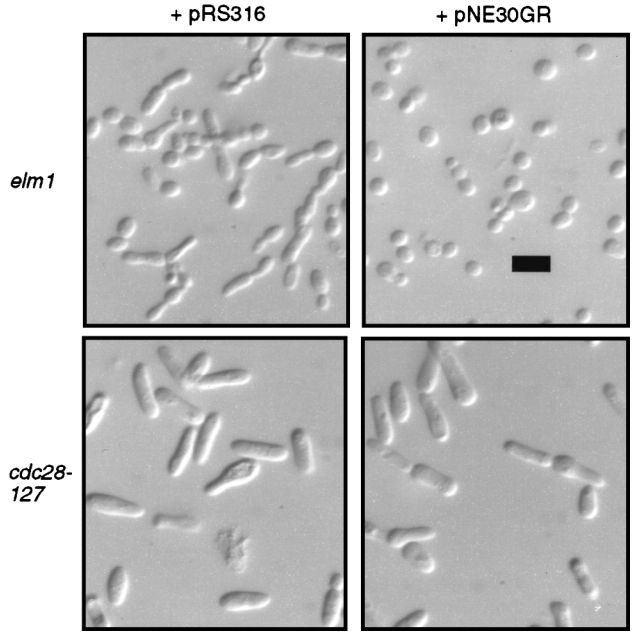

FIG. 5. Suppression of elongated cell morphology by *SEL2-1*. The *elm1-1* strain NEDN6d or the *cdc28-127* strain AY2287 was transformed to uracil prototrophy with pRS316 (empty vector) or pNE30GR (*SEL2-1* cloned in the same vector). Transformant colonies were grown overnight on selective agar medium, suspended on a slide in 1.2 M sorbitol, and visualized with differential interference contrast optics. Bar, 10 μm.

$Cdc28^{Y19F}$, in which the target tyrosine is replaced by a phenylalanine. Although $Cdc28^{Y19F}$ by itself resulted in slightly elongated cells, this phenotype was clearly distinguishable from that of *elm1 CDC28* cells. The presence of $Cdc28^{Y19F}$ suppressed the cell elongation phenotype induced by *elm1* (Fig. 6H), although apparently not as completely as did deletion of *SWE1* (Fig. 6E). This result further implicates the Hsl1-Swe1-Cdc28 pathway as a controlling factor for filamentous growth, at least when it is induced by *elm1* mutations. Analogous experiments showed $Cdc28^{Y19F}$ suppressed the cell elongation effects of *hsl1* mutations (42).

TABLE 2. Intergenic linkage data

Loci	Strains crossed	TT:NPD:PD[a]	Map distance (cM)[b]
HSL1-ELM1	NEY1494 × αDU	30:0:25	27.3
HSL1-PUT3	NEY2018 × NEY2065	11:1:3	56.7
HSL1-BUD2	NEY1494 × NEY2019	4:0:31	5.71
HSL1-GFA1	NEY2065 × NEY2020	2:0:50	1.92

[a] Tetratype (TT), nonparental ditype (NPD), parental ditype (PD).
[b] The map distance was calculated from the formula [50(TT + 6NPD)]/(TT + NPD + PD). cM, centimorgans.

The Hsl1-Swe1 pathway affects filamentous growth in otherwise wild-type cells. The invasive-growth response was examined in strains containing various mutations in the Hsl1-Swe1 pathway, to test whether this kinase cascade functions as a regulator of morphogenesis in response to specific external signals. Congenic strains were grown on rich medium for 2 days, at which time cells were washed off the surface of the plates to reveal the extent of invasive growth. The wild-type control strain underwent invasive growth as expected (Fig. 7A), although the response was much more extensive after 4 days of growth (data not shown). The *hsl1::LEU2* mutant exhibited a much greater extent of invasive growth than did wild type cells (Fig. 7A), with a response at 2 days similar to that of the maximal wild-type response at 4 days. Examination of colonies growing inside the agar medium showed the mutants to be much more elongated than wild-type cells undergoing invasive growth (Fig. 7B and C). Enhancement of invasive growth by the *hsl1* mutation was dependent on Swe1, because *swe1::URA3 hsl1::LEU2* double mutants were markedly reduced in their degree of invasive growth compared to the *hsl1::LEU2* single mutant (Fig. 7A, E, and H). The extent of invasive growth in the double mutant was the same as that observed in *swe1* single mutants and was noticeably less than wild-type cells (Fig. 7D and G). These data are again consistent with the hypothesis that inhibition of Cdc28 by Swe1 action is required for filamentous growth and that Hsl1 activity negatively regulates Swe1. The hypothesis suggests that dominant mutations of Hsl1, originally identified as suppressors of filamentous-growth characteristics induced by *elm1* mutations, also would inhibit invasive growth of otherwise wild-type cells. As predicted, the extent of invasive growth in strains bearing the dominant allele, *SEL2-1*, was significantly reduced compared to that in the wild-type strain (Fig. 7D and F).

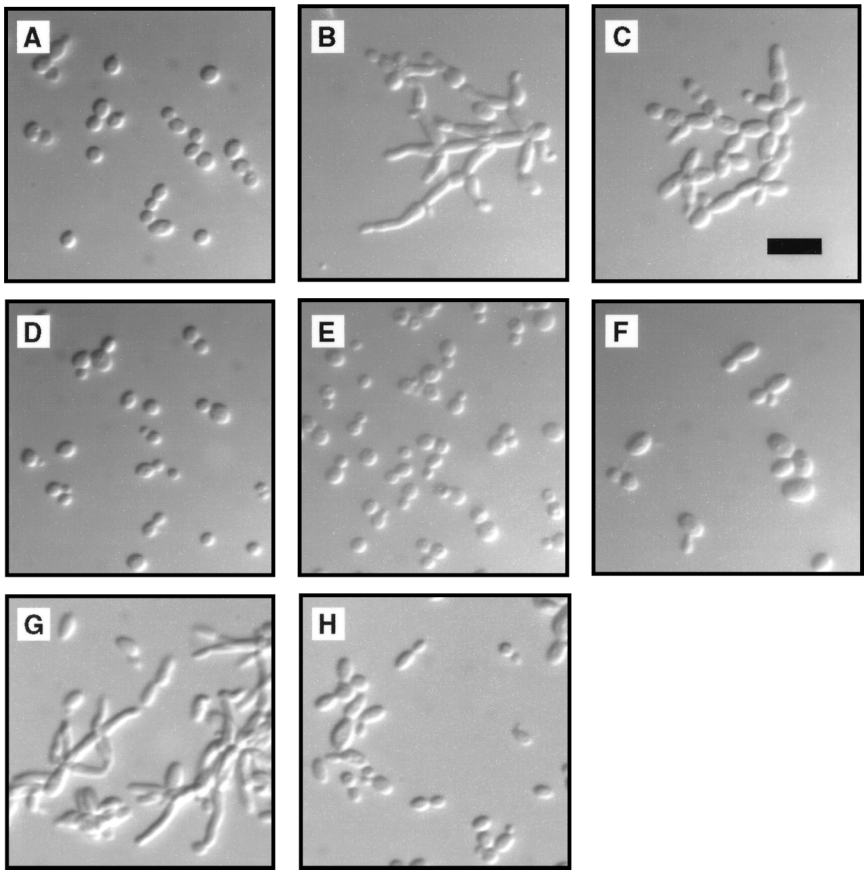

FIG. 6. Phosphorylation of *CDC28* by Swe1 is required for mutational induction of filamentous-growth characteristics. Strains were grown overnight on YPD plates, suspended in 1.2 M sorbitol, and visualized with differential interference contrast optics. (A) Strain NEY2340 (wild type). (B) Strain NEY2338 (*elm1::HIS3*). (C) Strain NEY2335 (*hsl1::LEU2*). (D) Strain NEY2344 (*swe1::URA3*). (E) Strain NEY2341 (*elm1::HIS3 swe1::URA3*). (F) Strain NEY2339 (*hsl1::LEU2 swe1::URA3*). (G) Strain AY2452 (*CDC28 elm1::HIS3* [p28Y19F-URAc]). (H) Strain AY2451 (*cdc28::LEU2a elm1::HIS3* [p28Y19F-URAc]). Bar, 10 μm.

***cdc28-127* is epistatic to mutations in the Hsl1-Swe1 pathway.** The effects of mutations in *HSL1* and *SWE1* regarding filamentous-growth characteristics and the invasive-growth response presumably are mediated by *CDC28*. This hypothesis predicts that the filamentous-growth characteristics resulting from *cdc28-127* would occur independent of whether the Hsl1-Swe1 pathway was functional. To test this hypothesis, the dominant allele *SEL2-1* was introduced into a *cdc28-127* strain. Although this mutation clearly suppressed the filamentous-growth characteristics in an *elm1-1* strain, there was no effect on the phenotype of the *cdc28-127* strain (Fig. 5). In addition, *SWE1* was deleted in a *cdc28-127* mutant strain. The double mutant displayed constitutive filamentous-growth characteristics identical to *cdc28-127* single mutants (data not shown), again indicating that the mutant Cdc28 protein is a downstream effector of filamentous-growth characteristics.

DISCUSSION

Filamentous-growth characteristics can be affected by alteration of Elm1, Hsl1, Swe1, or Cdc28. This study revealed that $Cdc28^{C127Y}$ simultaneously causes at least four cellular characteristics that are specific to the filamentous-growth form: simultaneous bud emergence, elongated cell shape, specifically altered bud site selection, and the ability to grow invasively in agar medium. The fact that so many specific aspects of filamentous-form cells result from this single amino acid substitution is unlikely to be coincidental. We suggest instead that wild-type cells undergoing filamentous growth in response to the normal environmental signals alter Cdc28 function in a way that is duplicated or mimicked by *cdc28-127*.

Identification of Cdc28 as a controlling factor in morphologic differentiation is expected from the known variations in cell cycle progression between filamentous-form and yeast-form cells (32). Kron et al. (32) proposed that a signalling pathway involving components of the Ste MAP kinase cascade is activated by environmental signals and results in inhibition of the G_2 activity of the Cdc28 complex. Cdc28 activity also was known previously to control cell morphology (35). The effects of $Cdc28^{C127Y}$ are consistent with these studies and indicate further that a modified Cdc28 complex can also mediate the bud site selection and invasive-growth properties of the filamentous form. Thus, the Cdc28 complex is proposed to be a central downstream regulator of filamentous-form differentiation (Fig. 8). The fact that $Cdc28^{C127Y}$ does not cause delayed cell separation might be explained by a separate signaling pathway being responsible for this filamentous growth characteristic. Alternatively, $Cdc28^{C127Y}$ may not fully mimic the CDK changes that occur normally during filamentous-form differentiation.

The Hsl1-Swe1 pathway also was implicated in control of filamentous growth, providing independent evidence that Cdc28 is a central regulator of this process. Although direct evidence that Hsl1 represses the activity of Swe1 by phosphor-

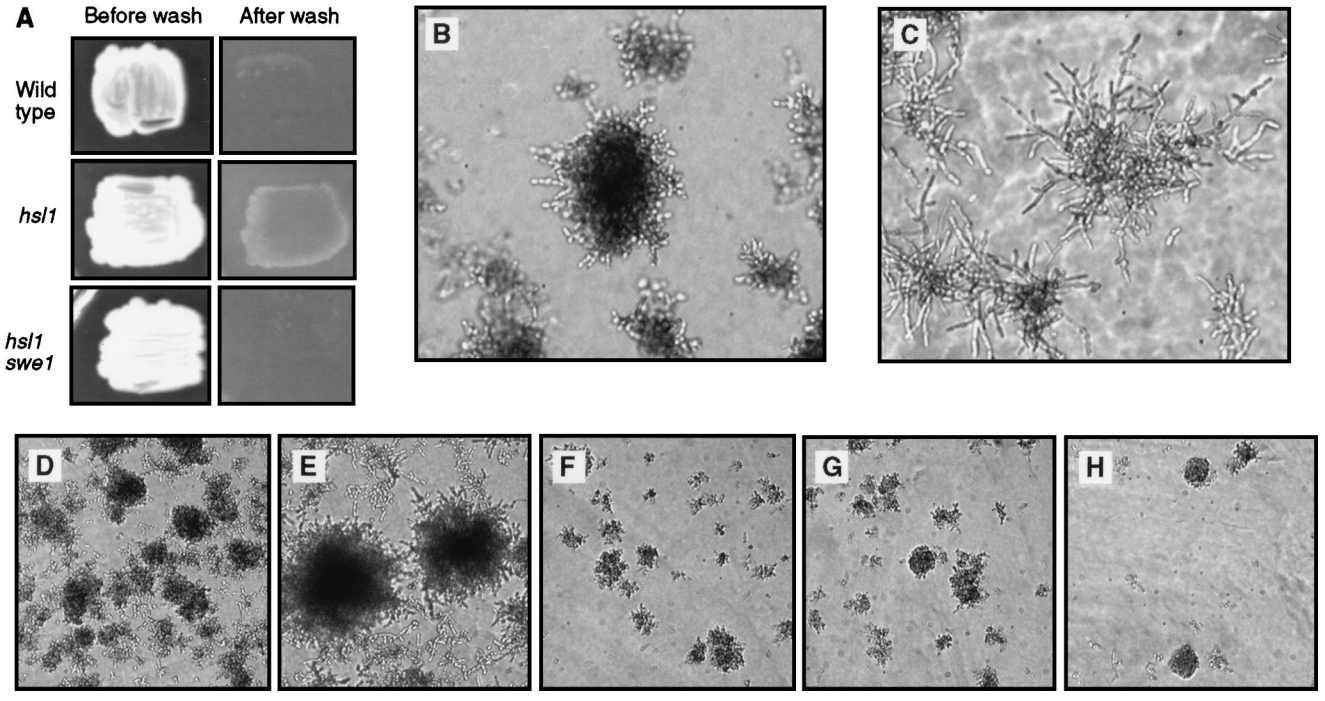

FIG. 7. Invasive growth is affected by mutations of the Hsl1-Swe1 pathway. (A) Invasive-growth assay. The indicated strains were grown for 2 days on YPD plates, and the cells were washed off of the surface of the plates. The strains are **a**DUL (wild type), NEY2335 (*hsl1::LEU2*), and NEY2339 (*hsl1::LEU2 swe1::URA3*). (B and C) Colonies growing underneath the agar, from the plates shown in panel A, photographed under an inverted microscope. (B) Strain **a**DUL (wild type). (C) Strain NEY2335 (*hsl1::LEU2*). (D to H) Colonies growing underneath the agar, all taken from a single YPD plate washed after 4 days of growth. In each of these panels, the photograph was taken from the densest area of invasive growth. (D) Strain NEY2340 (wild type). (E) Strain NEY2335 (*hsl1::LEU2*). (F) Strain NEY2353 (*SEL2-1*). (G) Strain NEY2344 (*swe1::URA3*). (H) Strain NEY2339 (*hsl1::LEU2 swe1::URA3*).

ylation is not available, there is ample genetic data suggesting that these two proteins function in a hierarchical cascade (42, 65). The effects of Swe1 are dependent on phosphorylation of Y19 of Cdc28, and in this instance the enzyme-substrate relationship has been defined (11). Thus, modification of Cdc28 is most likely to be the reason that mutations of *HSL1* and *SWE1* can impart filamentous-growth characteristics or repress those phenotypes. In this scenario, Swe1 is needed for filamentous-form growth by inhibiting Cdc28 whereas Hsl1 is required for yeast-form growth owing to its ability to inhibit Swe1.

Figure 8 presents a model suggesting that Elm1 functions upstream in a hierarchical cascade involving Hsl1, Swe1, and Cdc28. The following facts are consistent with this model. First, phosphorylation of Cdc28 residue 19 by the Hsl1-Swe1 pathway is necessary for *elm1* mutations to cause filamentous-growth characteristics. Second, dominant mutations in *HSL1*, expected to activate the protein, bypass the lack of Elm1. Third, deletion of *HSL1* causes a morphologic phenotype similar to that of *elm1* strains. These facts might also be explained by a variation of the depicted model, in which Elm1 and Hsl1 independently regulate the activity of Swe1. Consistent with either variation of the hypothesis, Hsl1 (6, 20) and Elm1 (67, 72) colocalize at the mother-bud neck.

The fact that *elm1*, *hsl1*, and *cdc28-127* mutations obviate the requirement for any of the multiple aspects of the normal filamentous-growth signals implicates these proteins as downstream regulators of the response. This conclusion is consistent with the finding that *ste7* and *ste20* mutations do not prevent the morphological effects of *ELM1* or *HSL1* deletion (48). The Hsl1-Swe1 pathway could be regulated as a downstream target of the Ste MAP kinase cascade including Ste12p, although currently there is no known evidence supporting a direct connection between these two signal transduction modules.

Some insight into Hsl1 function in filamentous-growth regulation might be gained from consideration of Nim1. In *S. pombe*, nitrogen starvation stimulates the mating pathway and results in rapid degradation of Nim1 (7, 21, 27, 74). Loss of Nim1 results in activation of Wee1, resultant phosphorylation of the Cdc28 homolog Cdc2 on tyrosine 15, and cell cycle arrest in G_2. In *S. cerevisiae*, *hsl1* mutants are sensitive to nitrogen concentration, so that increased nitrogen source suppresses the extreme elongated morphology observed in these mutants in stationary phase (65). Collectively, these data suggest a possible scenario in which Hsl1 degradation may occur in response to nutrient deprivation, thereby eliciting a Swe1-mediated delay in the G_2 phase of the cell cycle and stimulation of filamentous growth.

Two aspects of the suppression of *elm1* mutations by the presence of $Cdc28^{Y19F}$ remain to be explained. First is the fact that the suppressive effect of the nonphosphorylatable form of Cdc28 is not as strong as that resulting from deletion of *SWE1* (Fig. 6E and H). Thus, additional factors in this signaling pathway are likely to exist. Second is the fact that $Cdc28^{Y19F}$ was able to suppress *elm1* only when it was the sole form of Cdc28 in the cell (Fig. 6G and H). The presence of normal Cdc28 apparently interferes with the ability of $Cdc28^{Y19F}$ to perform whatever functions are necessary to restore yeast-form growth to the *elm1* mutant, although the reason for this effect currently is not known.

Possible filamentous-growth signals in nonmutant cells. Whether the filamentous-growth signalling pathway actually uses Elm1, Hsl1, and Swe1 is an open question. Several po-

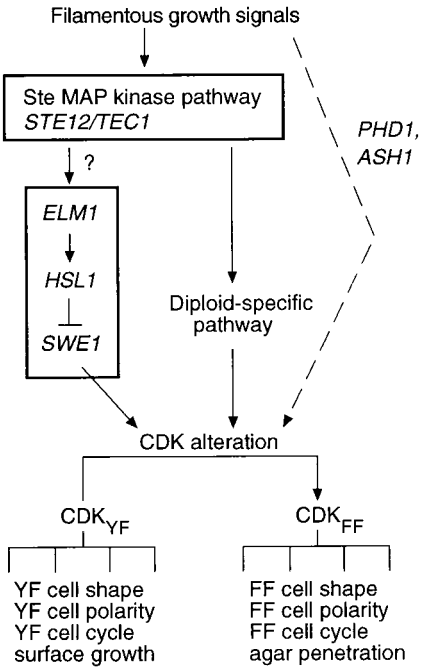

FIG. 8. Model for the role of the Cdc28 complex in control of filamentous growth. CDK_{YF} and CDK_{FF} suggest two slightly different activity states of the Cdc28 complex, which mediate different downstream effects. The Hsl1-Swe1 pathway, with Elm1 as a direct or indirect positive regulator of Hsl1, is proposed as a signal transduction module that can affect the change between CDK_{YF} and CDK_{FF}. At least one other means of affecting the change between CDK_{YF} and CDK_{FF} is proposed, because diploid cells undergo filamentous growth independent of Swe1 function. The Ste MAP kinase pathway is proposed as a possible upstream signaling module that affects the Hsl1-Swe1 pathway, although evidence of a direct connection between these modules is lacking, as noted by the question mark. The dotted line indicates the existence of possible alternative means of affecting the change between the CDK_{YF} and CDK_{FF} activity states, which may be mediated by other transcription factors providing morphologic differentiation functions that are partially redundant with Ste12p.

tential mechanisms are known that might alter cell cycle control to result in a spectrum of phenotypic changes similar to that induced by the mutations investigated in this study (for reviews, see references 23, 28, 49, and 73). Any one of these, or a combination, might be used in normal filamentous-growth signaling. The fact that invasive growth is compromised by deletion of *SWE1* (Fig. 7) suggests that in this instance the Hsl1-Swe1 pathway is in fact directly involved in filamentous-growth signaling.

Activity of the Hsl1-Swe1 pathway certainly cannot entirely explain filamentous-growth signaling, because *swe1*/*swe1* diploids and $Cdc28^{Y19F}$ strains both respond normally to the pseudohyphal growth signals (32). To explain the fact that filamentous growth in haploids is affected by Y19 phosphorylation whereas the response in diploids does not require this cascade, we suggest that redundant mechanisms exist for filamentous-growth signaling to Cdc28 (Fig. 8). Kron et al. (32) suggested that activation of the Ste MAP kinase pathway may produce an inhibitor of the Clb-Cdc28 complex that functions independently of Y19 phosphorylation. If such an inhibitor was not present in haploids, the Swe1 pathway might be required for invasive growth but not for pseudohyphal growth in diploids. Even if such redundant pathways do exist, however, both mechanisms could be dependent on the Ste MAP kinase pathway (Fig. 8), because disruption of this signal abrogates the filamentous-growth response in both haploids and diploids (37, 55). This issue is complicated significantly by the fact that partially redundant signaling pathways seem to regulate filamentous growth, for example those involving the transcriptional regulatory proteins Ash1, Ste12, and Phd1 (13). Additional genetic and biochemical network analysis is needed to identify connections between downstream signaling modules such as the Hsl1-Swe1 pathway and upstream modules such as that comprising the Ste MAP kinase cascade.

Mutations of *CLB2* constitutively cause filamentous-growth characteristics in some genetic backgrounds (1, 35), and Clb2 overexpression suppresses the morphologic effects of *cdc28-127*. These observations raise the possibility that decreased Cdc28-Clb activity is a general aspect of filamentous-growth signaling. Clb expression is regulated transcriptionally and by cell cycle-specific proteolytic degradation (29, 49). In addition, Cdc28-Clb function is inhibited by Sic1p (17, 62). Thus, downregulation of Cdc28-Clb as part of filamentous-growth signalling could occur by a variety of mechanisms. Another possibility is that expression of the G_1 cyclins could be altered so that the Cdc28-Cln complexes are hyperactive in filamentous-form cells compared to the yeast form. This condition is known to cause hyperpolarization of cell growth (35) and also to shorten the G_1 phase (49), so that the morphologic effects of Cln hyperactivation may be similar to those of reduced Clb function. Consistent with this hypothesis, mutations of the gene *GRR1*, which codes for a component of a complex that promotes Cln1 and Cln2 degradation (4, 5, 64), were isolated based on their ability to cause filamentous-growth characteristics (9, 10). Furthermore, *cln1 cln2* mutants are defective in filamentous growth (51). The Cln-Cdc28 and Clb-Cdc28 complexes are known to be functionally interrelated, for example by the fact that Clb2-Cdc28 inhibits transcription of *CLN1* and *CLN2* (2). Thus, changes in one phase of the cell cycle that result from a specific filamentous-growth signal are likely to have secondary implications throughout the cycle that contribute to morphologic differentiation.

As a last consideration regarding the mechanisms that might cause alteration of Cdc28 function so that filamentous-growth characteristics result, we expect that the changes will be subtle. Filamentous-form cells grow at nearly the same rate as do yeast-form cells (8, 32) and are tightly regulated in terms of cell size and shape. Drastic alterations in Cdc28 function would cause significant growth rate defects and frequent aberrant divisions. The uniform nature of filamentous-form cells argues that although Cdc28 activity may be altered, it still performs all essential functions, albeit with slightly different kinetics. Higher eukaryotes can regulate morphogenesis and cellular differentiation by modifying the cell cycle program (19). Further analysis of the *S. cerevisiae* cell division cycle and its control in filamentous growth is likely to provide significant insights into how cell division in more complex organisms can be modulated to accomplish specific functions during cellular differentiation.

ACKNOWLEDGMENTS

We thank D. Lew, M. Brandriss, H.-O. Park, C. Styles, and M. Gentzsch for supplying strains and/or plasmids.

This work was supported by National Science Foundation grants MCB-9319028 and MCB-9604247.

REFERENCES

1. **Acurio, A., S.-H. Ahn, and S. J. Kron.** 1998. Personal communication.
2. **Amon, A., M. Tyers, B. Futcher, and K. Nasmyth.** 1993. Mechanisms that help the yeast cell cycle clock tick: G2 cyclins transcriptionally activate G2 cyclins and repress G1 cyclins. Cell **74:**993–1007.
3. **Ausubel, F. M., R. Brent, R. E. Kingston, D. D. Moore, J. A. Smith, J. G. Seidman, K. Struhl.** 1989. Current protocols in molecular biology. John Wiley & Sons, Inc., New York, N.Y.

4. **Barral, Y., S. Jentsch, and C. Mann.** 1995. G_1 cyclin turnover and nutrient uptake are controlled by a common pathway in yeast. Genes Dev. **9:**399–409.
5. **Barral, Y., and C. Mann.** 1995. Degredation des cyclines G1 et differenciation cellulaire chez *Saccharomyces cerevisiae*. C. R. Acad. Sci. Paris **318:**43–50.
6. **Barral, Y., M. Parra, S. Bidingmaier, and M. Snyder.** 1998. Nim1 homologs of *S. cerevisiae* link cell-cycle progression to proper organization of the peripheral cytoskeleton, abstr. 79, p. 84. *In* Abstracts of the 1998 Yeast Genetics and Molecular Biology Meeting. Genetics Society of America, College Park, Md.
7. **Belenguer, P., L. Pelloquin, M. L. Oustrin, and B. Ducommun.** 1997. Role of the fission yeast nim1 protein kinase in the cell cycle response to nutrient signals. Biochem. Biophys. Res. Commun. **232:**204–208.
8. **Blacketer, M. J., C. M. Koehler, S. G. Coats, A. M. Myers, and P. Madaule.** 1993. Genetic control of dimorphism in *Saccharomyces cerevisiae*: involvement of the novel protein kinase homologue Elm1p and protein phosphatase 2A. Mol. Cell. Biol. **13:**5567–5581.
9. **Blacketer, M. J., P. Madaule, and A. M. Myers.** 1994. The *Saccharomyces cerevisiae* mutation *elm4-1* facilitates pseudohyphal differentiation and interacts with a deficiency in phosphoribosylpyrophosphate synthase activity to cause constitutive pseudohyphal growth. Mol. Cell. Biol. **14:**4671–4681.
10. **Blacketer, M. J., P. Madaule, and A. M. Myers.** 1995. Genetic analysis of morphologic differentiation in *S. cerevisiae*. Genetics **140:**1259–1275.
11. **Booher, R. N., R. J. Deshaies, and M. W. Kirschner.** 1993. Properties of *Saccharomyces cerevisiae* wee1 and its differential regulation of $p34^{CDC28}$ in response to G_1 and G_2 cyclins. EMBO J. **12:**3417–3426.
12. **Broach, J. R., J. N. Strathern, and J. B. Hicks.** 1979. Transformation in yeast: development of a hybrid cloning vector and isolation of the CAN1 gene. Gene **8:**121–133.
13. **Chandarlapaty, S., and B. Errede.** 1998. Ash1, a daughter cell-specific protein, is required for pseudohyphal growth of *Saccharomyces cerevisiae*. Mol. Cell. Biol. **18:**2884–2891.
14. **Chant, J.** 1994. Cell polarity in yeast. Trends Genet. **10:**328–333.
15. **Chant, J., and I. Herskowitz.** 1991. Genetic control of bud site selection in yeast by a set of gene products that constitute a morphogenetic pathway. Cell **65:**1203–1212.
16. **Cook, J. G., L. Bardwell, S. J. Kron, and J. Thorner.** 1996. Two novel targets of the MAP kinase Kss1 are negative regulators of invasive growth in the yeast *Saccharomyces cerevisiae*. Genes Dev. **10:**2831–2848.
17. **Donovan, J. D., J. H. Toyn, A. L. Johnson, and L. H. Johnston.** 1994. $P40^{SDB25}$, a putative CDK inhibitor, has a role in the M/G1 transition in *Saccharomyces cerevisiae*. Genes Dev. **8:**1640–1653.
18. **Drubin, D. G.** 1996. Origins of cell polarity. Cell **84:**335–344.
19. **Edgar, B. A., and C. F. Lehner.** 1996. Developmental control of cell cycle regulators: a fly's perspective. Science **274:**1646–1652.
20. **Edgington, N. P., and A. M. Myers.** Unpublished data.
21. **Feilotter, H., P. Nurse, and P. G. Young.** 1991. Genetic and molecular analysis of cdr1/nim1 in *Schizosaccharomyces pombe*. Genetics **127:**309–318.
22. **Friefelder, D.** 1960. Bud formation in *Saccharomyces cerevisiae*. J. Bacteriol. **80:**567–568.
23. **Futcher, B.** 1996. Cyclins and the wiring of the yeast cell cycle. Yeast **12:** 1635–1646.
24. **Gavirias, V., A. Andrianapolous, C. J. Gimeno, and W. E. Timberlake.** 1996. *Saccharomyces cerevisiae* TEC1 is required for pseudohyphal growth. Mol. Microbiol. **19:**1255–1263.
25. **Gimeno, C. J., and G. R. Fink.** 1994. Induction of pseudohyphal growth by overexpression of *PHD1*, a *Saccharomyces cerevisiae* gene related to transcriptional regulators of fungal development. Mol. Cell. Biol. **14:**2100–2112.
26. **Gimeno, C. J., P. O. Ljungdahl, C. A. Styles, and G. R. Fink.** 1992. Unipolar cell divisions in the yeast *S. cerevisiae* lead to filamentous growth: regulation by starvation and RAS. Cell **68:**1077–1090.
27. **Hayles, J., and P. Nurse.** 1992. Genetics of the fission yeast *Schizosaccharomyces pombe*. Annu. Rev. Genet. **26:**373–402.
28. **Hoyt, M. A.** 1997. Eliminating all obstacles: regulated proteolysis in the eukaryotic cell cycle. Cell **91:**149–151.
29. **King, R. W., R. J. Deshaies, J.-M. Peters, and M. W. Kirschner.** 1996. How proteolysis drives the cell cycle. Science **274:**1652–1659.
30. **Koehler, C. M., and A. M. Myers.** 1997. Serine-threonine protein kinase activity of Elm1p, a regulator of morphologic differentiation in *Saccharomyces cerevisiae*. FEBS Lett. **408:**109–114.
31. **Kron, S. J., and N. A. R. Gow.** 1995. Budding yeast morphogenesis: signaling, cytoskeleton and cell cycle. Curr. Opin. Cell Biol. **7:**845–855.
32. **Kron, S. J., C. A. Styles, and G. R. Fink.** 1994. Symmetric cell division in pseudohyphae of the yeast *Saccharomyces cerevisiae*. Mol. Biol. Cell **5:**1003–1022.
33. **Kübler, E., H.-U. Mösch, S. Rupp, and M. P. Lisanti.** 1997. Gpa2p, a G-protein α-subunit, regulates growth and pseudohyphal development in *Saccharomyces cerevisiae* via a cAMP-dependent mechanism. J. Biol. Chem. **272:**20321–20323.
34. **Lew, D. J., N. J. Marini, and S. I. Reed.** 1992. Different G1 cyclins control the timing of cell cycle commitment in mother and daughter cells of the budding yeast *S. cerevisiae*. Cell **69:**317–327.
35. **Lew, D. J., and S. I. Reed.** 1993. Morphogenesis in the yeast cell cycle: regulation by Cdc28 and cyclins. J. Cell Biol. **120:**1305–1320.
36. **Lew, D. J., T. Weinert, and J. R. Pringle.** 1997. Cell cycle control in *Saccharomyces cerevisiae*, p. 607–695. *In* J. R. Pringle, J. R. Broach, and E. W. Jones (ed.), The molecular and cellular biology of the yeast *Saccharomyces*. Cell cycle and cell biology. Cold Spring Harbor Laboratory Press, Plainview, N.Y.
37. **Liu, H., C. A. Styles, and G. R. Fink.** 1993. Elements of the yeast pheromone response pathway required for filamentous growth of diploids. Science **262:** 1741–1744.
38. **Liu, H., C. A. Styles, and G. R. Fink.** 1996. *Saccharomyces cerevisiae* S288C has a mutation in *FLO8*, a gene required for filamentous growth. Genetics **144:**967–978.
39. **Lo, W. S., and A. M. Dranginis.** 1998. The cell surface flocculin Flo11 is required for pseudohyphae formation and invasion by *Saccharomyces cerevisiae*. Mol. Biol. Cell **9:**161–171.
40. **Lorenz, M. C., and J. Heitman.** 1997. Yeast pseudohyphal growth is regulated by GPA2, a G protein α homolog. EMBO J. **16:**7008–7018.
41. **Lorenz, M. C., and J. Heitman.** 1998. The MEP2 ammonium permease regulates pseudohyphal differentiation in *Saccharomyces cerevisiae*. EMBO J. **17:**1236–1247.
42. **Ma, X.-J., Q. Lu, and M. Grunstein.** 1996. A search for proteins that interact genetically with histone H3 and H4 amino termini uncovers novel regulators of the Swe1 kinase in *Saccharomyces cerevisiae*. Genes Dev. **10:**1327–1340.
43. **Madhani, H. D., and G. R. Fink.** 1997. Combinatorial control required for the specificity of yeast MAPK signaling. Science **275:**1314–1316.
44. **Madhani, H. D., C. A. Styles, and G. R. Fink.** 1997. MAP kinases with distinct inhibitory functions impart signaling specificity during yeast differentiation. Cell **91:**673–684.
45. **Marczak, J. E., and M. C. Brandriss.** 1989. Isolation of constitutive mutants affecting the proline utilization pathway in *Saccharomyces cerevisiae* and molecular analysis of the *PUT3* transcriptional activator. Mol. Cell. Biol. **9:**4696–4705.
46. **Mösch, H.-U., and G. R. Fink.** 1997. Dissection of filamentous growth by transposon mutagenesis in *Saccharomyces cerevisiae*. Genetics **145:**671–684.
47. **Mösch, H.-U., R. L. Roberts, and G. R. Fink.** 1996. Ras2 signals via the Cdc42/Ste20/mitogen-activated protein kinase module to induce filamentous growth in *Saccharomyces cerevisiae*. Proc. Natl. Acad. Sci. USA **93:**5352–5356.
48. **Myers, A. M.** Unpublished data.
49. **Nasmyth, K.** 1993. Control of the yeast cell cycle by the Cdc28 protein kinase. Curr. Opin. Cell Biol. **5:**166–179.
50. **Nasmyth, K.** 1996. At the heart of the budding yeast cell cycle. Trends Genet. **12:**405–412.
51. **Oehlen, L., and F. R. Cross.** 1998. Potential regulation of ste20 function by the Cln1-Cdc28 and Cln2-Cdc28 cyclin-dependent protein kinases. J. Biol. Chem. **273:**25089–25097.
52. **Park, H.-O., J. Chant, and I. Herskowitz.** 1993. *BUD2* encodes a GTPase-activating protein for Bud1/Rsr1 necessary for proper bud-site selection in yeast. Nature **365:**269–274.
53. **Pringle, J. R., and L. H. Hartwell.** 1981. The *Saccharomyces cerevisiae* cell cycle, p. 97–142. *In* J. N. Strathern, E. W. Jones, and J. R. Broach (ed.), Molecular biology of the yeast *Saccharomyces*. Cold Spring Harbor Laboratory Press, Cold Spring Harbor, N.Y.
54. **Richardson, H. E., D. J. Lew, M. Henze, K. Sugimoto, and S. I. Reed.** 1992. Cyclin-B homologs in *Saccharomyces cerevisiae* function in S phase and in G2. Genes Dev. **6:**2021–2034.
55. **Roberts, R. L., and G. R. Fink.** 1994. Elements of a single MAP kinase cascade in *Saccharomyces cerevisiae* mediate the two developmental programs in the same cell type: mating and invasive growth. Genes Dev. **8:**2974–2985.
56. **Roberts, R. L., H.-U. Mösch, and G. R. Fink.** 1997. 14-3-3 proteins are essential for RAS/MAPK cascade signaling during pseudohyphal development in *S. cerevisiae*. Cell **89:**1055–1065.
57. **Rose, M. D., F. Winston, and P. Heiter.** 1990. Methods in yeast genetics. A laboratory course manual. Cold Spring Harbor Laboratory Press, Plainview, N.Y.
58. **Rothstein, R.** 1991. Targeting, disruption, replacement, and allele rescue: integrative DNA transformation in yeast. Methods Enzymol. **194:**281–301.
59. **Russell, P., and P. Nurse.** 1987. The mitotic inducer $nim1^+$ functions in a regulatory network of protein kinase homologs controlling initiation of mitosis. Cell **49:**569–576.
60. **Russell, P., and P. Nurse.** 1987. Negative regulation of mitosis by $wee1^+$, a gene encoding a protein kinase homolog. Cell **49:**559–567.
61. **Sambrook, J., E. F. Fritsch, and T. Maniatis.** 1989. Molecular cloning: a laboratory manual, 2nd ed. Cold Spring Harbor Laboratory Press, Cold Spring Harbor, N.Y.
62. **Schwob, E., T. Bohm, M. D. Mendenhall, and K. Nasmyth.** 1994. The B-type cyclin kinase inhibitor $p40^{SIC1}$ controls the G1 to S transition in *S. cerevisiae*. Cell **79:**233–244.
63. **Sikorski, R. S., and P. Hieter.** 1989. A system of shuttle vectors and yeast host strains designed for efficient manipulation of DNA in *Saccharomyces cerevisiae*. Genetics **122:**19–27.

64. **Skowyra, D., K. L. Craig, M. Tyers, S. J. Elledge, and J. W. Harper.** 1997. F-box proteins are receptors that recruit phosphorylated substrates to the SCF ubiquitin-ligase complex. Cell **91:**209–219.
65. **Tanaka, S., and H. Nojima.** 1996. Nik1: a Nim1-like protein kinase of *S. cerevisiae* interacts with the Cdc28 complex and regulates cell cycle progression. Genes Cells **1:**905–921.
66. **Tedford, K., S. Kim, D. So, K. Stevens, and M. Tyers.** 1997. Regulation of the mating pheromone and invasive growth responses in yeast by two MAP kinase substrates. Curr. Biol. **7:**228–238.
67. **Thomas, C., and A. M. Myers.** Unpublished data.
68. **Tzagoloff, A., A. Akai, and F. Foury.** 1976. Assembly of the mitochondrial membrane system. XVI. Modified form of the ATPase proteolipid in oligomycin-resistant mutants of *S. cerevisiae*. FEBS Lett. **65:**391–396.
69. **Wallis, J. W., G. Chrebet, G. Brodsky, M. Rolfe, and R. Rothstein.** 1989. A hyper-recombination mutation in *S. cerevisiae* identifies a novel eukaryotic topoisomerase. Cell **58:**409–419.
70. **Ward, M. P., C. J. Gimeno, G. R. Fink, and S. Garrett.** 1995. *SOK2* may regulate cyclic AMP-dependent protein kinase-stimulated growth and pseudohyphal development by repressing transcription. Mol. Cell. Biol. **15:** 6854–6863.
71. **Watzele, G., and W. Tanner.** 1989. Cloning of the glutamine:fructose-6-phosphate amidotransferase gene from yeast. J. Biol. Chem. **264:**8753–8758.
72. **Wei, W., and I. Herskowitz.** 1998. Identification of genes that are required for bud morphogenesis and the activation of G2 CLB/CDC28 activity, abstr. 314, p. 203. *In* Abstracts of the 1998 Yeast Genetics and Molecular Biology Meeting. Genetics Society of America, College Park, Md.
73. **Wittenberg, C., and S. I. Reed.** 1996. Plugging it in: signaling circuits and the yeast cell cycle. Curr. Opin. Cell Biol. **8:**223–230.
74. **Wu, L., and P. Russell.** 1997. Roles of Wee1 and Nim1 protein kinases in regulating the switch from mitotic division to sexual development in *Schizosaccharomyces pombe*. Mol. Cell. Biol. **17:**10–17.